

Article

Controls on the Spatial Distribution of Trace Metal Concentrations along the Bedrock-Dominated South Fork New River, North Carolina

Jerry R. Miller ^{1,*}, Xaviera Watkins ², Thomas O'Shea ³ and Cynthia Atterholt ⁴¹ Department of Geosciences & Natural Resources, Western Carolina University, Cullowhee, NC 28723, USA² Independent Researcher, 3140 Carver School Road, Winston Salem, NC 27105, USA; xavierawatkins1@outlook.com³ Bunnell-Lammons Engineering, Inc., Greenville, SC 29615, USA; taoshea.geo@outlook.com⁴ Department of Chemistry & Physics, Western Carolina University, Cullowhee, NC 28723, USA; atterholt@email.wcu.edu

* Correspondence: jmiller@wcu.edu; Tel.: +1-828-227-2269

Abstract: In marked contrast to alluvial rivers, few studies have examined the physical and geochemical controls on the spatial distribution of toxic trace metals along bedrock channels. This study examined the factors controlling the geographical pattern of selected trace metal (Cu, Cr, and Zn) concentrations along the bedrock-dominated channel of the South Fork New River (SFNR). The SFNR is located in the Blue Ridge Physiographic Province of North Carolina, and is representative of many rivers in mountainous terrains that are often subjected to the influx of toxic trace metals from historic and contemporary mining operations. The topography of the SFNR's channel bed is highly variable and can be subdivided into pool and shallow bedrock reaches. The latter contained localized cascades characterized by topographically higher bedrock ribs that are separated by topographic lows, both of which are oriented oblique to flow. Accumulations of bed sediments are predominantly associated with the transverse bedrock ribs that generate high hydraulic roughness. Except for a few localized zones of enrichment, sediment-associated trace metal concentrations tended to vary within a narrow range of background values over the 36 km study reach. Elevated trace metal concentrations were closely linked to zones of high Fe and Mn concentrations, and were associated with pools located within or immediately downstream of bedrock cascades. The elevated concentrations of the metals appear to be derived from the erosion of lithologic units within the cascades that contain sulfidic layers or zones of mafic mineral enrichment, and which are known to occur in the underlying bedrock. Once eroded, these minerals and/or rock fragments were deposited within low-velocity zones created by the transverse ribs or within downstream pools. The enrichment of trace metals downstream of the cascades may also be due to the formation of Fe and Mn oxyhydroxides as turbulent flows aerate river waters as they traverse the cascades. Chemically reactive fine-grained (<63 µm) sediments had a relatively limited influence on the downstream variations in metal concentrations, presumably because the channel bed sediments are composed primarily of sand-sized and larger particles. Although a principal component analysis (PCA) suggested that reach-scale variations in channel and valley morphology may have partly influenced downstream variations in trace metal concentrations, the geographical patterns were primarily controlled by local geological and geomorphic factors associated with the bedrock cascades. The design of future sampling programs along such coarse-grained, bedrock rivers should consider the significance of these local controls on trace metal storage to effectively characterize and interpret downstream patterns in metal concentrations.



Citation: Miller, J.R.; Watkins, X.; O'Shea, T.; Atterholt, C. Controls on the Spatial Distribution of Trace Metal Concentrations along the Bedrock-Dominated South Fork New River, North Carolina. *Geosciences* **2021**, *11*, 519. <https://doi.org/10.3390/geosciences11120519>

Academic Editors: Javier Lillo, Maria De La luz Garcia Lorezo and Jesus Martinez-Frias

Received: 18 October 2021

Accepted: 13 December 2021

Published: 17 December 2021

Publisher's Note: MDPI stays neutral with regard to jurisdictional claims in published maps and institutional affiliations.



Copyright: © 2021 by the authors. Licensee MDPI, Basel, Switzerland. This article is an open access article distributed under the terms and conditions of the Creative Commons Attribution (CC BY) license (<https://creativecommons.org/licenses/by/4.0/>).

Keywords: bedrock rivers; trace metal contamination; sediment deposition; geomorphic controls; New River

1. Introduction

Anthropogenic activities, particularly during and following the industrial revolution, have led to the widespread contamination of river channels and floodplains by toxic trace metals (which have historically been referred to as heavy metals consisting of metallic elements with a density $> \sim 6 \text{ g/cm}^3$). The long-term ecological and human health effects of toxic trace metals are largely dependent on the quantity, concentrations, and rate at which they are discharged to the environment, but can be significant because of their long residence times in sediments and soils (often measured in thousands of years [1]), their toxicity, even at low concentrations, and their potential to be bioaccumulated in plants and animals [2]. While toxic trace metals in the environment are derived from a wide range of sources, both contemporary and historic mining operations, and the subsequent processing of metal ores, has led to the release of enormous quantities of metal-enriched particulate wastes (tailings). During the past four decades, the potential impacts of mining operations on aquatic ecosystems has been extensively documented, both from an academic perspective and from the perspective of remediating a contaminated site [1–7]. Such studies have shown that 90–95% of the trace metal load in rivers characterized by natural Eh and pH conditions occurs in association with particulate matter [8,9]. Thus, the physical (geomorphic) controls on sediment-associated metal dispersal have been a significant component of studies aimed at documenting the transport and fate of trace metals in riverine environments. The overwhelming majority of these geomorphic-geochemical investigations have focused on alluvial channels in which the channel bed and bank materials are composed of loose unconsolidated sediments.

In marked contrast to alluvial channels, the physical and geochemical analysis of bedrock rivers has been limited. Geomorphically, bedrock rivers differ from their alluvial counterparts in that the quantity of sediment supplied to the river is less than the channel's sediment transporting capacity. Consequently, bedrock is either continuously exposed along the channel floor, or is discontinuously covered by unconsolidated sediment, forming a patchwork of alluvial deposits [10–12]. The spatial characteristics of these alluvial patches have become a recent topic of considerable interest because (1) the incision of the bedrock is thought to be a key process controlling landscape evolution [13,14], and (2) the rate of incision reflects a balance between the abundance of coarse bed material that promotes erosion by impacting and abrading the exposed bedrock and the thickness of the alluvium that can cover and protect the bedrock from abrasion [12,15]. Bedrock rivers also differ from alluvial rivers in that the topography of the channel floor is highly variable, exhibiting a wide range of often randomly distributed features that may strongly influence channel roughness and, therefore, the geographical location of sediment deposition [11,12].

The above investigations into the factors controlling the incision of bedrock rivers have necessarily focused on the processes of coarse-grained sediment transport and deposition. The transport and fate of chemically reactive, fine-grained sediments, and their associated trace metal concentrations, is comparatively unknown. This is in spite of the fact that bedrock channels are ubiquitous in mountainous terrains, and numerous mines, particularly small-scale, historic mining operations, are located along mountainous headwater streams characterized by bedrock channels. In fact, there are more than 500,000 abandoned or inactive hard rock mines in the U.S. alone [16,17], the majority of which have, and continue, to generate effluent and tailings wastes.

The primary objective of this study was to explore the factors controlling the spatial variations in sediment-associated trace metal concentrations within the South Fork New River (SFNR), a bedrock river in North Carolina that is representative of many rivers within the Blue Ridge Physiographic Province of the southeastern U.S. as well as many other mountainous terrains. More specifically, the analysis focuses on how changes in channel morphology (shape), including the distribution of selected bedrock features sculpted into the channel floor, have influenced fine-grained sediment and trace metal deposition along the river over a range of spatial scales. The objectives of the study were accomplished by interpreting a combination of geomorphic, cartographic, and geochemical data using a

variety of approaches that examine the linkages between geomorphic and sedimentological parameters and selected trace metal concentrations.

2. Study Area

The South Fork New River

The SFNR heads along the western flank of the Blue Ridge Mountains which locally exceed 1525 m in elevation. The region is characterized by a humid continental climate with an average annual precipitation of 124 cm that varies little throughout the year; a minimum monthly average precipitation of 8.3 cm occurs in December, whereas a high of 12.4 cm occurs in May [18]. The average annual temperature is 10.8 °C; the hottest average summer temperatures occur in July (26.6 °C), whereas the coldest average monthly temperatures occur in December (−6.05 °C).

From its headwaters, the river flows in a northeasterly direction for approximately 201 km from near Boone, North Carolina to its confluence with the North Fork New River near the Virginia border. The watershed of the SFNR encompasses an area of 1950 km², which generates a daily mean discharge of 15.4 m³/s. The river's valley is characterized by an alternating sequence of narrow reaches possessing spatially limited alluvial deposits (surfaces) separated by reaches dominated by relatively wide valleys with extensive floodplains, many of which are used for agriculture.

Several small, historic mines exist within the watershed. The most significant is the Ore Knob Copper Mine located approximately 13 km east of Jefferson, North Carolina (Figure 1). The ore body consists of a 2.4–5.5 m thick, steeply dipping mineralized vein that extends for more than 1220 m along the geological contact between a gneiss and biotite schist [19]. Mineralogically, the vein is dominated by pyrrhotite, pyrite, chalcopyrite, quartz, biotite and amphiboles [19,20]. The deposit was first intensively mined between about 1873 to 1883 [21], when 11,500 t of Cu ore was produced. Mining at the site subsequently ceased until the mine reopened in the late 1950s; from 1957 to 1962 the mine produced Cu, Au, and Ag using froth flotation and a cyanide leaching process [18–20].

Waste materials from the mining operations were placed in a tailings pile that was constructed by building a 21 m-high, 215 m-wide earthen dam across Ore Knob Branch, a headwater tributary to Peak Creek. The tailings pile contains an estimate 550,480 m³ of waste materials that cover an area of approximately 8.1 ha [21]. Surface water from the upstream watershed, in addition to precipitation, migrated into and through the waste materials before flowing downstream into Peak Creek which subsequently enters the SFNR. The mine's impact on sediment and water quality of the SFNR has not been studied in detail.

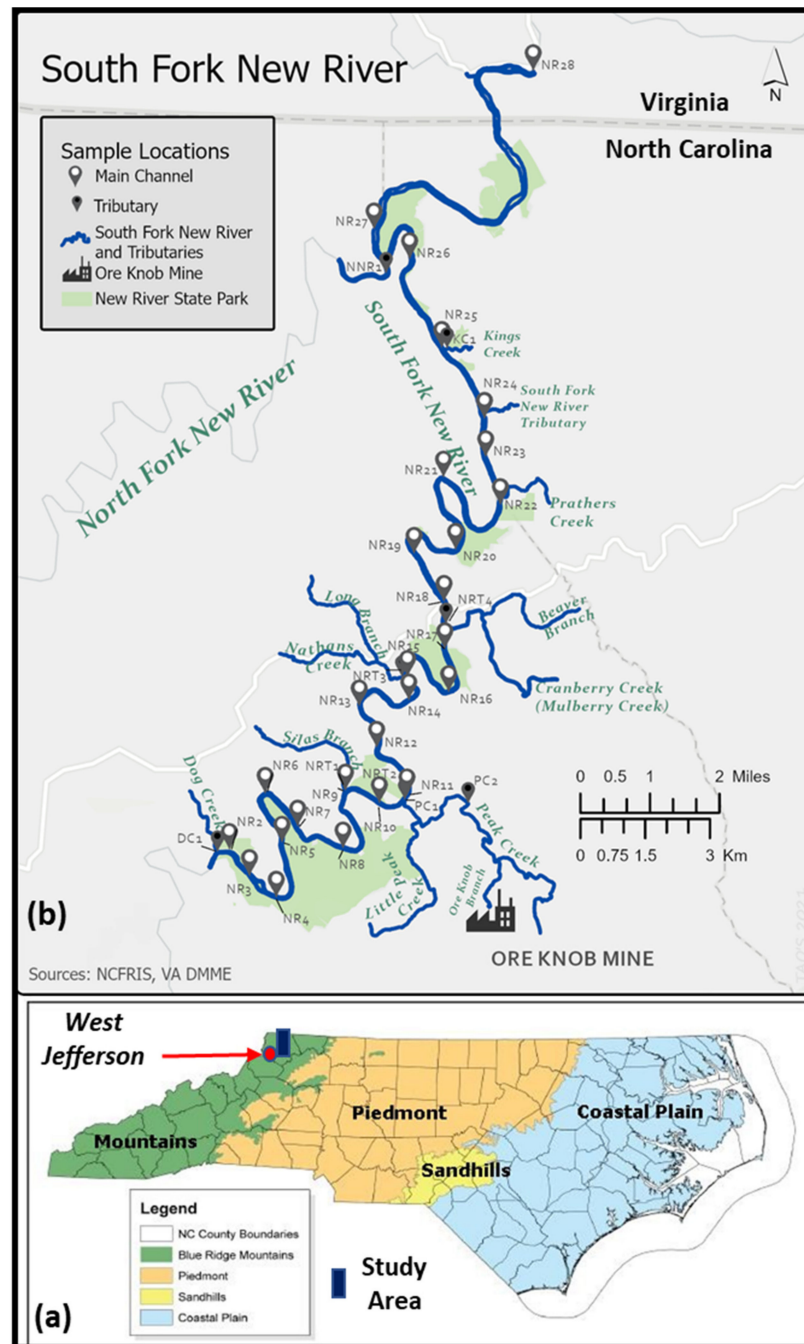


Figure 1. (a) Map showing the location of the studied reach of the South Fork New River in North Carolina; (b) location of the Ore Knob Mine and the sampling sites along the South Fork New River. North Carolina Map from the <https://triaddentalstudio.com/reasons-to-move-to-greensboro/> (accessed on 6 August 2021).

3. Materials and Methods

3.1. Sample Collection

A total of 25 sediment samples were collected in August 2018 at approximately 1.5-km intervals along the 36 km study reach of the SFNR between Dog Creek and the North Fork New River during low (base) flow conditions (Figure 1). Samples were also obtained from major tributaries including Peak Creek (which drains the Ore Knob Mine site), Dog Creek, Cranberry Creek, and Kings Creek, among others (Figure 1). At each sampling site, the sediments (<2 mm in size) were collected from approximately the upper 5 cm of the channel bed at multiple locations across the channel and composited (combined)

to reduce field variance. At many sites, unconsolidated bed sediments were limited and irregularly covered the channel floor; the loose <2 mm sediment fraction primarily occurred downstream of, or adjacent to, large boulders and bedrock obstructions, and/or was associated with small sand bars developed along the channel margins. At these sites, samples were primarily collected from multiple locations downstream of the obstructions to flow. All samples were placed in polyethylene containers that were then added to plastic bags and shipped to Western Carolina University (WCU) for analysis.

3.2. Geomorphic and Geologic Data

Geomorphic data were collected to describe channel and valley morphology at various spatial scales along the study reach. Specific parameters included channel width (m) and slope (km/km), valley width (m), and the type of channel reach (pool vs. bedrock). The distance of the sampling site from bedrock cascades (topographic ridges that obliquely traversed the channel and created rapids) was also determined, along with the general type of bedrock underlying the reach. The latter was determined from a 1:250,000 scale, state geologic map of North Carolina [22].

The geomorphic data, in general, were measured in the laboratory from 1 m resolution LiDAR DEMs acquired from the North Carolina Flood Risk Information System [23], and North Carolina OneMap [22]. Analyses were performed using ArcGIS Pro software. The mapping was performed using the UTM coordinate system, zone 17N, and the NAD 83 datum. An initial step in the process was to create a route feature for the SFNR. Route features allow the user to consistently define the beginning and end of a line segment and to calculate distance measurements along the feature. The developed route feature for the SFNR served as the reference for all distance measurements in our tabular dataset. The locate features along route tool in ArcGIS Pro was then used to manually measure minimum distances of the sampling site from bedrock cascades, and to calculate the average slope of the channel bed (as described below).

The determination of valley widths required the delineation of the boundary between the valley floor and the hillslope. The boundary was based on abrupt changes in the spacing of the 1 m contour lines created using the high-resolution LiDAR DEM to define the valley toe. Valley widths were subsequently determined by creating perpendicular transect lines at 10-m intervals along the study reach of SFNR using the generate transects along lines tool. A subset of these transects that intersected the sampling locations was subsequently selected; the rest were discarded. The cross sections at each of the sampling sites were then manually adjusted to measure channel width using the calculate geometry tool. This process was repeated to measure channel width; however, aerial imagery (from Maxar Technologies) was used to determine channel widths (Figure S1).

Channel slope at each of the sampling locations was determined by creating an elevation profile for the length of the entire 36 km study reach. The SFNR route was used to determine the x coordinate along the channel and the 1 m resolution LiDAR DEM was used to determine the y coordinate (elevation). Average slope for each sample location was then determined from a plot of the x and y coordinates for a 20 m length of the SFNR centered on the sample location. Whenever sudden changes in slope were observed, the data range was adjusted to measure the average slope most representative of the sample location.

Aerial imagery (from Maxar Technologies) was used to manually identify and outline bedrock cascades, thereby creating a polygon. Cascades were defined as channel reaches where bedrock or boulders obliquely traversed the channel and breached the water surface creating significant and easily visible turbulence. Polygon features were subsequently generalized and converted to center points. The locate features along route tool was then used to determine the minimum downstream distance of each sample site from a bedrock cascade. These measurements are approximate but allow the researcher to make comparisons across sample locations.

The SFNR can also be subdivided into two distinct reach types: bedrock and pools (Figures 2 and S2). Reach type was mapped along the river on aerial imagery and used

to define the reach type at each sample site. The reach type was then verified on the basis of field notes/observations. In general, pools were characterized by relatively deep, slower moving water devoid of large boulders or exposed bedrock that breached the water surface. These reaches are devoid of significant turbulence at the water surface. In contrast, bedrock reaches are characterized by relatively shallow water depths (allowing the channel bed to be visible on aerial imagery), but faster moving water characterized by frequently turbulent conditions at the water surface. Contained within the bedrock reaches are cascades, characterized by an alternating sequence of topographic highs (ribs) and lows that obliquely traversed the river (Figure S2).



Figure 2. (a,b) Stream reaches classified as pools along the South Fork New River; (c,d) stream reaches classified as bedrock reaches (without transverse ribs).

3.3. Analytical Methods

A total of six metals (including Cd, Cr, Cu, Ni, Pb, and Zn) were selected for geochemical analysis on the basis of their potential ecological impacts. Cadmium and Ni concentrations were consistently below detection. Lead (Pb) concentrations were below the level of detection at about 35% of the sampled sites. Thus, these elements will not be discussed further; rather, we will focus on Cr, Cu, and Zn as representative trace metals. Iron (Fe) and Mn were also analyzed due to their ubiquitous occurrence in riverine environments, and their potential to serve as significant scavengers of trace metals [24–26]. In addition, Al, Co, Si, and Ti concentrations were determined for their possible use as proxies of particle grain size and indicators of sediment provenance [4,27].

Prior to geochemical analysis, the sediment samples were air dried, and sieved using a nylon mesh to obtain the <2 mm sediment fraction. A subsample of the sieved sediment was then ground with a mortar and pestle into fine (<63 μm) particles. The ground sediments were subsequently placed in a plastic XRF sample cup to which a Mylar film had been fitted to its bottom, and secured with a plastic cap. Sediment was then added and packed in the cup, after which a small piece of cotton was placed on top to securely hold the sediment in the sampling cup. The samples were then analyzed by means of a METEK Spectro Xepos energy-dispersive, X-ray fluorescence (ED-XRF) spectrometer. Ten samples were measured simultaneously along with 2 external standards, including OREAS 930 and USGS SGR-1b. Comparison of the measured concentrations to the external standards showed that the measured elemental concentrations were within $\pm 10\%$. The concentrations determined by XRF represent total elemental concentrations within the sediments, including both bioavailable and non-bioavailable metal fractions.

The percent of fine sediment (<63 μm) was also determined for each sample. The analysis involved the addition of ~5 g of sediment to a 50 mL beaker. Approximately 40 mL of deionized water was subsequently added to the beaker along with 5 mL of 10% sodium pyrophosphate dispersing agent. The mixture was stirred and allowed to sit for at least 24 h. After re-stirring the sample mixture, the grain-size distribution of the <2 mm size fraction was determined at 0.5 phi intervals using a Mastersizer 2000 particle size analyzer (Malvern Instruments, Malvern, UK) at WCU. The average of the three samples was used to represent the percent of fine sediment (<0.063 mm) and percent of fine sand (0.063 mm to 0.250 mm) in the sample. The level of detection of fine sediment was determined to be 2% for silt and clay.

The approximate organic matter content of the samples was determined by means of loss-on-ignition (LOI). The sediment samples were initially dried (~70 °C) for 6–8 h. Then ~5–10 g of sediment was added to a ceramic crucible, after which it was massed and recorded. The crucible was heated at 550 °C for 6 h, and placed into a desiccator and allowed to cool. The LOI was calculated as:

$$\frac{(\text{Sediment Sample} - \text{Heated Sediment Sample}) \text{ g}}{(\text{Sediment Sample}) \text{ g}} \times 100 = \text{LOI} \% \quad (1)$$

Once the LOI had been determined, the organic matter content in the sample was estimated by multiplying the LOI values by 0.55 to adjust for the effects of particle size and furnace temperature [28].

3.4. Statistical Methods

A wide range of statistical methods were used in the analysis (e.g., correlation analyses, bivariate scatter plots, Tukey's boxplots, and principal components analysis). These analyses were conducted using IBM SPSS Statistics 26. The normality of the geochemical data was assessed using a Shapiro–Wilk normality test and normal Q-Q plots. Aluminum, Mn, Fe, Co, and Si data were non-normally distributed at the 95% confidence level. Thus, correlation analyses relied on the Kendall's tau b test, which is a robust method with respect to normality. Regression analyses relied upon the robust least trimmed square regression approach, which was performed using R programming language. Plots and general data manipulations were conducted using Microsoft Excel and Origin 9.0. Specifics of the utilized statistical methods are provided in more detail below.

4. Results and Discussion

4.1. Influence of Sediment-Metal Relations on Downstream Trace Metal Patterns

Spatial variations in metal concentrations along river channels is perhaps one of the most frequently generated and analyzed datasets in the geochemical analysis of river systems. Such spatial data are used for a wide spectrum of purposes, ranging from the exploration of economic ore deposits to the determination of contaminant sources, to the identification of contaminant hotspots requiring remediation. Variations in concentration along alluvial rivers have generally been attributed to five factors, including (1) the proximity to, and magnitude of inputs from point and diffuse metal sources, (2) geochemical processes that promote metal precipitation or dissolution, including redox sensitivity scavenger elements such as Fe and Mn, (3) the partitioning of sediment-associated metals into discrete geomorphic features and deposits by hydraulic processes, (4) metal dilution by relatively "clean" or non-reactive sediments (e.g., quartz), and (5) biological uptake [29]. All five of these controlling factors are related, in part, to how they occur within the sediments, eliciting an analysis of sediment-trace metal relations. Correlation analysis is commonly used to explore these relations.

The geochemical data for several of the analyzed elements were non-normally distributed. Thus, a Kendall tau b correlation analysis was used to assess the relations between the three examined trace metals (Cu, Cr, and Zn) and the sediment's content of chemically reactive constituents. The latter included fine-grained sediment (silt- and clay-sized

particles, <63 μm), organic matter (OM) and the concentrations of Fe and Mn, which are indicators of Fe and Mn oxyhydroxides [24]. General descriptive statistics of the collected data used in the correlation analyses are presented in Supplementary Materials Table S1. With regards to Cu, Cr, and Zn concentrations in the collected channel bed sediments are all statistically correlated to one another as well as to Fe and Mn at the $p < 0.01$ level (Table 1). In addition, all three trace metals (Cu, Cr, and Zn) are correlated at the $p < 0.01$ level to the fine sediment content of the deposits. Fe is also related to the fine sediment content of the samples, whereas Mn is not, the latter indicating that (1) the spatial controls on Mn concentrations differ from those of fine sediment, and (2) Mn is also associated with larger, sand-sized particles.

Table 1. Kendall tau b correlation coefficients between trace metal concentrations and sediment characteristics.

$n = 25$	Fine Sed.	OM	Al	Cr	Cu	Fe	Mn	SI	Zn
Fine Sed.	1								
OM	0.000	1							
Al	0.539 **	−0.003	1						
Cr	0.434 **	−0.003	0.400 **	1					
Cu	0.588 **	−0.067	0.457 **	0.591 **	1				
Fe	0.475 **	−0.084	0.420 **	0.767 **	0.691 **	1			
Mn	0.249	0.205	0.140	0.567 **	0.518 **	0.667 **	1		
Si	−0.611 **	−0.037	−0.553 **	−0.553 **	−0.651 **	−0.560 **	−0.320 *	1	
Zn	0.523 **	−0.118	0.413 **	0.613 **	0.551 **	0.767 **	0.593 **	−0.513 **	1

Statistically significant correlations at the $p < 0.01$ (**) or $p < 0.05$ (*) level.

It is important to recognize that while the above Kendall tau b correlation analyses suggest that the toxic metals are associated with fine sediments, the channel bed sediments were dominated by coarse materials. In fact, about half of the collected samples possessed less than 2% silt and clay (the level of detection). An alternative approach to assess the compositional controls on the concentrations of toxic metals is through the use of lithogenic elements (e.g., Al, Si, and Ti) as proxies for grain size [4,30]. Aluminum and Ti, for example, are often associated with clay minerals and other phyllosilicates; thus, their concentrations are positively correlated to the quantity of clay- and silt-sized sediment in the deposits. In contrast, Si (associated with sand-sized and larger particles of quartz and feldspar, among other silicates) tends to be negatively correlated to the amount of fine sediment in the deposits. Kendall tau b correlation analyses show that Al exhibits a good positive correlation ($R^2 = 0.54$, $p < 0.01$) with the fine sediment content of the channel bed deposits of the SFNR, whereas Si exhibited the expected negative correlation ($R^2 = -0.61$, $p < 0.01$) with the amount of fine sediment in the samples (Table 1). Ti, which is often associated with oxides and heavy minerals associated with clay minerals, exhibited a weaker correlation ($R^2 = 0.33$, $p < 0.5$) with fine sediment (not shown).

The positive correlation of fine sediment to Al, and its negative correlation to Si generally makes the Al/Si ratio a particularly effective proxy for grain size [4,30–32]. In the case of the SFNR, Al and Si are, in fact, inversely related to one another ($R^2 = 0.77$), and the Al/Si ratio increases with the sediment's fine sediment content ($R^2 = 0.48$, $p < 0.01$) (Figure 3). It appears, then, that both Al and Si can be used as a proxy for sediment grain size and composition.

Downstream variations in the quantity of fine sediment and organic matter in the SFNR's channel bed sediment, as well as its Mn and Fe contents, are shown in Figure 4a,b. Concentrations of these chemically reactive substances are similar between most sampling sites, with a few notable exceptions. These exceptions, as is usual, were identified using Tukey's box-and-whisker plots [30,33–35], wherein the median value is assumed to represent the geochemical baseline for the dataset, and the upper and lower whiskers represent the range of background values. This median-based approach to the assessment of background is applicable to non-normally distributed data [35]. The baseline and 75th percentile values for Al/Si ratios, organic matter, Mn, and Fe for the SFNR are shown in

Table 2. Al/Si ratios were used because many of the sites possessed non-detectable values (<2%) of fine sediment. There were no outliers for Mn and Fe; however, Site 26 was an outlier for Al/Si (Figure 4e). Given that we are concerned in this study with the identification of sites with relatively high concentrations of reactive substances, sites containing Mn, Fe, and Al/Si values within the upper quartile (75th percentile) were also identified. In the case of Mn, these sites included NR 8–10, NR 15, NR 21, NR 25, and NR 26. With the exception of Site 15, the Fe concentrations were also within the upper quartile at these same sites.

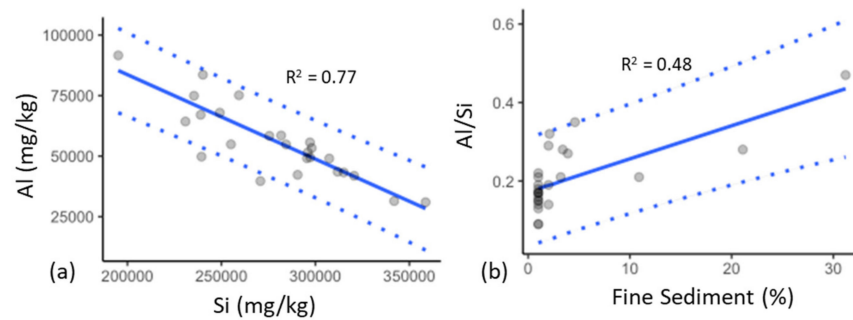


Figure 3. (a) Plot showing the relation between Al and Si for channel bed sediments from the South Fork New River (SFNR); (b) dependence of Al/Si on the cumulative percent of fine sediment (silt + clay) in the channel bed.

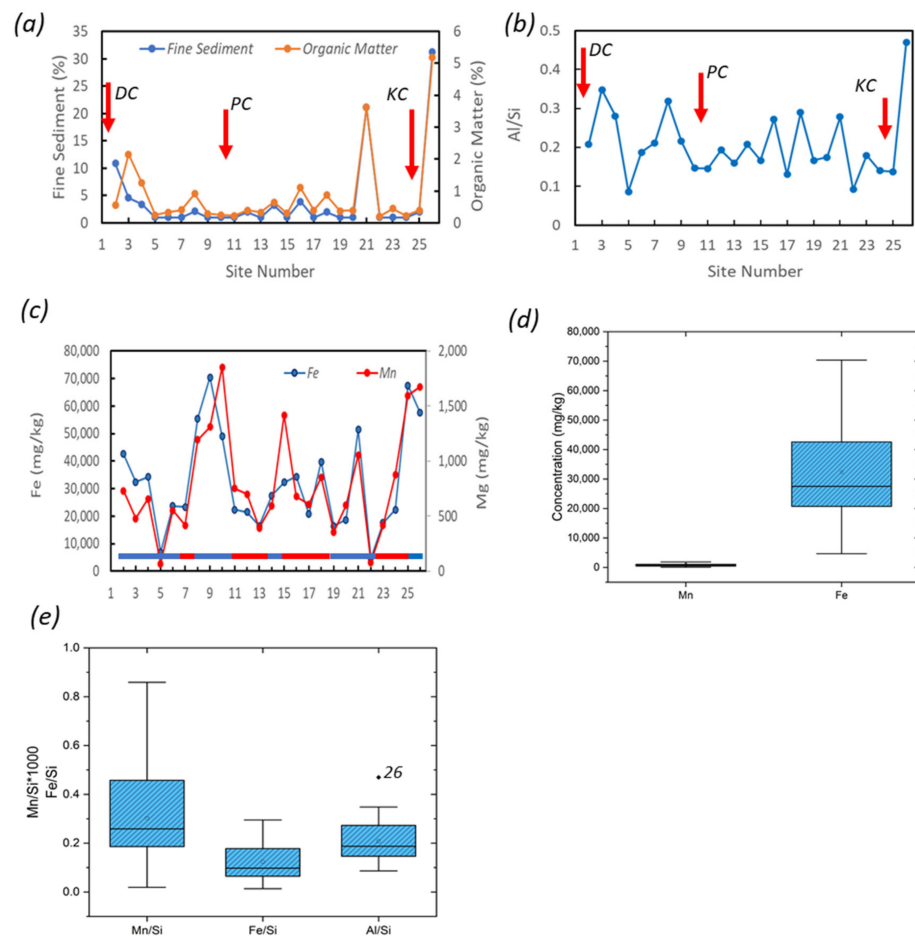


Figure 4. Downstream variations in fine sediment and organic matter content (a), Al/Si ratio (b), Mn and Fe concentrations, (c); lines beneath plot in 'c' represent distribution of pool (blue) and bedrock (red) reaches. Tukey's box-and-whisker plots for Mn and Fe (d) and Mn/Si, Fe/Si, and Al/Si (e). Larger tributaries are shown by red arrows. DC—Dog Creek; PC—Peak Creek (draining the Ore Knob Mine); CC—Cranberry Creek; KC—Kings Creek.

Table 2. Baseline (median), background (whisker), and 75th percentile concentrations determined using Tukey’s box-and-whisker plots.

Parameter	Baseline Value (mg/kg)	Background Range (mg/kg)	75th Percentile
Cr	19.09	19.09–75.67	62.78
Cu	12.62	3.67–36.59	22.97
Zn	55.27	2.17–133.36	73.63
Fe	27,522	4676–70,362	45,753
Mn	679	70–1852	1056
Organic Matter	0.4	0.2–1.25	0.87
Al/Si	0.18	0.086–0.348	0.28

The toxic trace metal (Cu, Cr, Pb, Zn) concentrations along the SFNR (Figure 5) were variable, and exhibit no systematic downstream trends. As expected from the correlation analyses, reaches characterized by high concentrations of one toxic metal generally possessed high concentrations of the other (and vice versa), suggesting a similar source and behavior within the river. We hypothesized that variations in toxic metal concentrations reflected, in part, differences in the abundance of chemically reactive, silt and clay-sized particles in the channel bed sediment, as is generally true for alluvial rivers. An advantage of using a proxy element to assess the influence of grain size is that the toxic metal data can be normalized by the concentration of the proxy, thereby allowing for the effects of sediment grain size and composition on trace metal concentrations to be minimized. However, the application of proxy ratio data must be used with some degree of caution as the concentration of elemental proxies can be influenced by factors other than grain size, including the maturity of the sediment (degree of weathering), diagenesis, biogenic alterations and provenance [30,32]. Herein, we used Si as a proxy for grain size due to its relatively high (negative) correlation to fine sediment (Table 1). Figure 5c shows that downstream variations in trace metal ratios with respect to Si. The downstream patterns, including sites with elevated Si normalized values (Figure 5c) are similar to those observed for the bulk concentrations (Figure 5a), indicating that factors other than grain size influence metal concentrations. Outlier concentrations consistently occurred at sites NR 9 (Cu, Cr), NR 21 (Cu, Pb), NR 25 (Zn), and NR 26 (Cu, Zn, Pb, Cr). Site NR 8 also exhibited relatively high values of Cr. Interestingly, these sites also exhibited Mn and Fe concentrations within the upper quartile of the analyzed samples. Site 26 also exhibited relatively high Al/Si ratios indicative of elevated fine sediment contents, while Site NR 21 possessed elevated organic matter contents. In the sections below, we examine some of the possible controls on the observed variations in sediment composition and trace metal concentrations.

4.2. Controls on the Spatial Variations in Metal Concentrations along the South Fork New River (SFNR)

4.2.1. Potential Influence of Provenance on Spatial Variations in Metal Concentrations

Geographical patterns in metal concentrations, and the reactive sediments to which they are sorbed, are often related to the proximity of the reach to, and the magnitude of influx from, a natural or anthropogenic source. Studies dating back to the 1970s [7,36–38] have shown that spatial patterns in concentration caused by human activities can be particularly pronounced. For example, metal influx from point sources of contamination, including mining operations, are often characterized by an abrupt downstream increase in toxic metal concentrations upon reaching the source, followed by a systematic downstream decline with distance from the source as a result of a combination of physical, chemical, and biological processes [37]. As noted in the description of the study area, the Ore Knob Mine, which was listed in 2009 as a Superfund site, is located within the Peak Creek watershed, which flows into the SFNR between sampling points NR 10 and NR 11 (Figure 1). State and federal agencies suggested that a short reach of the SFNR downstream of its confluence with Peak Creek may have been contaminated by acid mine drainage and

toxic trace metals [21,39]. However, geographical patterns in metal contents documented during this study showed no significant increase in trace metal concentrations immediately downstream of Peak Creek (Figure 5). Moreover, geochemical data from the lower reaches of Peak Creek showed that trace metal concentrations were similar to baseline values measured along the SFNR. It follows, then, that sediment-associated trace metal inputs from the Ore Knob Mine via Peak Creek have had little influence on the overall spatial distribution of toxic trace metals along the SFNR. This argument is supported by Manning–Whitney U tests that compared the metal concentrations (and the Si normalized concentrations) upstream of Peak Creek (sampling Sites NR 2 through NR 10), which are thought to be devoid of any significant inputs of anthropogenic metals, to those downstream of Peak Creek (NR 10 through NR 26). The results showed metal concentrations between the two channel reaches were similar at the 95% confidence level (Table S2). The lack of significant impact may be related to (1) dilution of trace metals in water and sediments from Peak Creek upon entering the much larger SFNR, and (2) the positive effects of site remediation activities associated with the Superfund cleanup process which began in 2011 (Table S3).

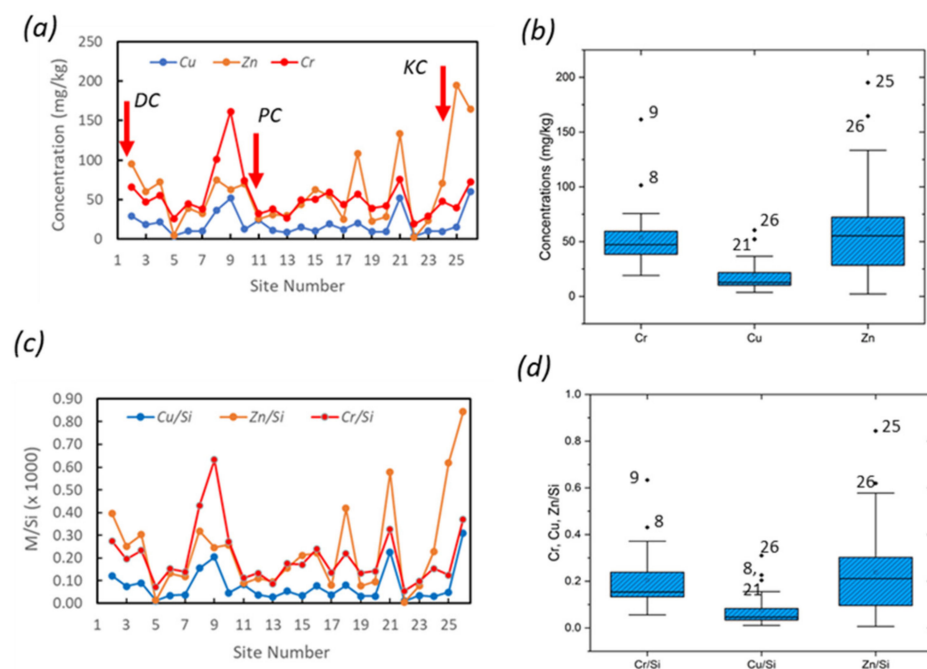


Figure 5. Downstream variations in (a) Cr, Cu, and Zn concentrations; (b) Tukey’s box-and-whisker plots of Cr, Cu, and Zn showing sites characterized by concentrations that exceed local base level; (c) Si normalized Cr, Cu, and Zn concentrations, and (d) Tukey’s box-and-whisker plots of Si normalized Cr, Cu, and Zn concentrations showing sites characterized anomalous values. Larger tributaries are shown by red arrows. DC—Dog Creek; PC—Peak Creek (draining the Ore Knob Mine); KC—Kings Creek.

Miller and Mackin [40] argued that downstream variations in sediment-associated metal concentrations along the Little Tennessee River in North Carolina were controlled, in part, but the erosion and influx of sulfide minerals from sulfidic layers within the underlying bedrock. More specifically, zones of relatively high metal concentrations were partly attributed to increases in bedrock outcrops along the river (which is also located in the Blue Ridge Physiographic Province). The SFNR differs from the Little Tennessee River in that bedrock exposures occur along the entire study reach of the SFNR; thus, differences in the extent of exposed bedrock are less likely to influence metal concentrations. It is possible, however, that the erosion of minerals and/or rock fragments from different bedrock types influence sediment-associated metal concentrations. The channel bed within the study reach is underlain primarily by three bedrock units including a muscovite-biotite gneiss, an amphibolite, and a biotite granitic gneiss (Figure 6, see Table S4 for descriptions).

Local outcrops of mica schist and meta-ultramafic serpentinites also occur along the river, both of which contain sulfidic zones and are enriched in heavy minerals. A Kruskal–Wallis test was used to determine if metal concentrations (Cr, Cu, Fe, Mn, Zn) of the sediments differed as a function of the underlying type of bedrock (only the first three rock units, for which there were sufficient sample numbers, were used in the analysis). The results suggest that there was no significant ($p < 0.05$) difference in metal concentrations across the different bedrock units (Table S5). However, the results of this analysis should be used with a high degree of caution because of the scale (1:250,000) of the mapped bedrock units, and the potential for mineral grains to be moved downstream to other sites.

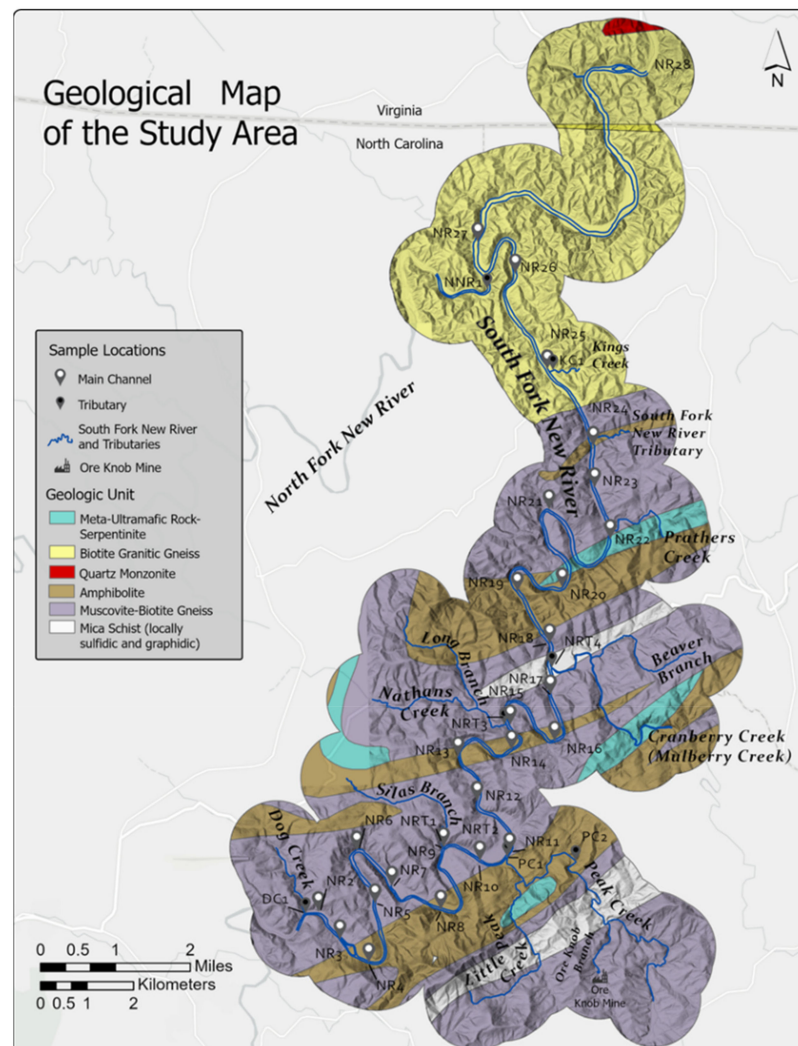


Figure 6. Geologic map of the study area. Extracted from the 1:250,000 geologic map of North Carolina [22].

An alternative approach to assess the influence of provenance on sediment composition is to examine the relations between selected lithogenic elements. Herein, Al/Si ratios (characterizing siliclastic minerals) were plotted against Mn and Fe (Figure 7) as well as Ti and Co. Sampling sites NR 9, NR 10, and NR 25 consistently displayed anomalous Fe, Mn, Ti, and Co values that did not plotted along the trend line (Figure 7). Site 15 also exhibited dissimilar Al/Si vs. Mn and Ti values (Figure 7). These data suggest that variations in bedrock composition led to localized anomalous inputs of Mn and Fe, probably in the form of mafic minerals (e.g., olivine, pyroxene, amphibole and various oxides and sulfides) that are known to be enriched within localized “layers” of the bedrock within the regions bedrock [22,41]. Interestingly, sites NR 9, NR 10, and NR 15 are characterized by pools

containing deeper, slower moving water located immediately downstream of bedrock reaches. These bedrock reaches containing cascades characterized by multiple ribs of resistant bedrock that extend downstream for tens of meters, and that obliquely traverse the channel bed (Figure 8). The sediment sample at Site NR 25 was collected from a deeper, low flow area of a bedrock reach.

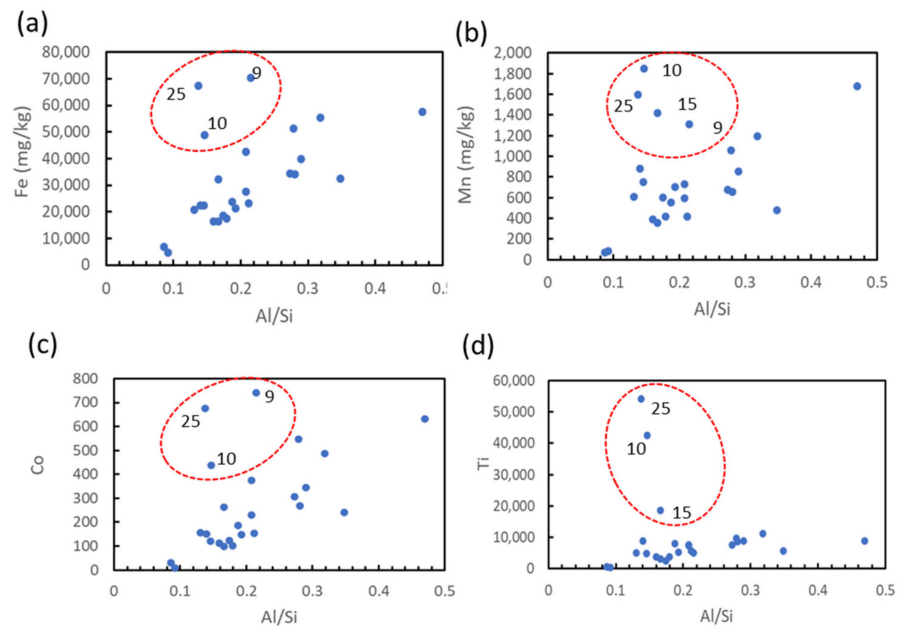


Figure 7. Scatter plots between Al/Si ratios and Fe (a), Mn (b), Co (c), and Ti (d). Outlier sampling sites are shown by the red-dashed circle.

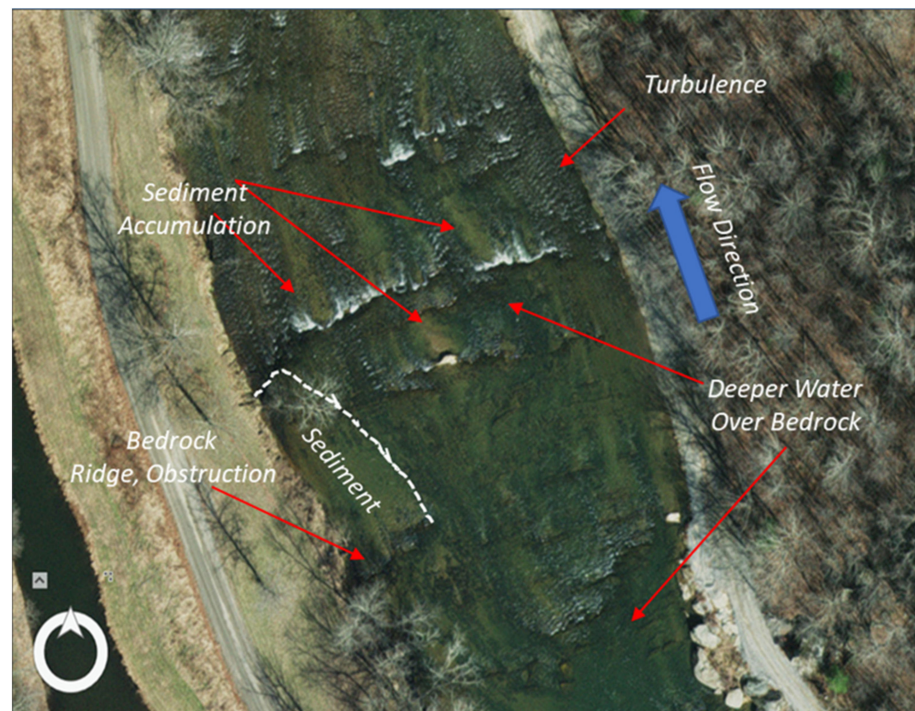


Figure 8. Reach containing a bedrock cascade showing effect of localized transverse ribs on flow turbulence and sediment deposition (image from NC Center for Geographic Information and Analysis, 6 December 2018. Available: NC One Map, <https://www.nconemap.gov/pages/imagery> (accessed on 6 August 2021).

Goode and Wohl [12] argued that along the Ocoee River and other streams in the Blue Ridge Physiographic Province, transversely oriented bedrock ribs, similar to the ribs that form the cascades along the SFNR, were related to localized variations in the erodibility of the underlying bedrock which were caused by changes in its lithologic and/or structural characteristics. Moreover, the formation of the ribs led to local increases in stream gradients and, therefore, stream powers, thereby promoting the erosion of the underlying bedrock. As rib developed progressed, the increase in stream power was offset by increases in hydraulic roughness, resulting in local erosional-depositional feedback processes whose magnitude varied with rock erodibility and which promoted rib/cascade formation. In the case of the SFNR, we speculate that the ribs associated with the cascades represent similar localized zones of erosionally resistant bedrock, that locally served as an anomalous source of relatively high concentrations of Mn and Fe (as well as Co and Ti). Once the Mn- and Fe-containing minerals and/or rock fragments had been eroded, they were transported downstream and deposited within deeper, slower moving pools within the bedrock reach (e.g., Site NR 25) or within downstream stream segments classified as pools (e.g., at sites NR 8–10).

The association between high Fe and Mn concentrations with bedrock cascades may not be exclusively related to the erosion of the bedrock. The localized precipitation of Fe and Mn oxyhydroxides along streams and rivers as a result of changing redox conditions has been widely recognized for more than four decades, and is often attributed to zones of increased turbulence that result in increased oxygen content of the water [26,27,42]. It may also be related to the infiltration and re-emergence of water (and groundwater) from fractured bedrock exposed in the channel floor. Jankowski [42], for example, found that subsurface longwall mining in the vicinity of the Waratah Rivulet in Australia led to subsidence and fracturing of the riverbed, which allowed surface waters to flow into and through the underlying sandstones. As the waters passed through the bedrock, water–rock interactions led to increased dissolved concentrations of Zn, Co, and Ni. When these waters re-emerged, in conjunction with groundwaters, they were quickly oxidized, leading to the precipitation of Fe and Mn oxyhydroxides, which then sorbed other metals. We speculate that as water approaches the cascades, which are topographically higher than the immediate downstream reach, water is forced into and through the bedrock (Figure S3). Its re-emergence downstream could result in the preferential precipitation of Fe and Mn oxyhydroxides, a process that could potentially be supplemented by the localized changes in redox conditions resulting from the turbulence and aeration of surface waters during flow through the cascades. Figure 9 provides some preliminary data to support this hypothesis. The concentrations of Fe, and to a much lesser degree, Mn tend to decrease downstream from the cascades before increasing again. It is worth noting, however, that the data were not collected downstream from a specific cascade, but represent the general distance of the sampling sites from multiple cascades. Thus, this potential phenomenon requires additional study.

4.2.2. Localized, Geomorphic Influences on Metal Concentrations

Numerous studies have demonstrated that along alluvial rivers with deformable (erodible) bed and banks, trace metal concentrations tend to vary over a range of spatial scales. At the local scale, trace metals are often preferentially partitioned into specific channel bed features (e.g., pools, riffles, and point bars) based on the size and density of the particles with which they are associated and the flow conditions that occur over the deposits [7,26,43–45]. Large (reach) scale variations have also been documented, as discussed in more detail below, that are related to changes in channel and valley morphology (width, slope, and dimensions).

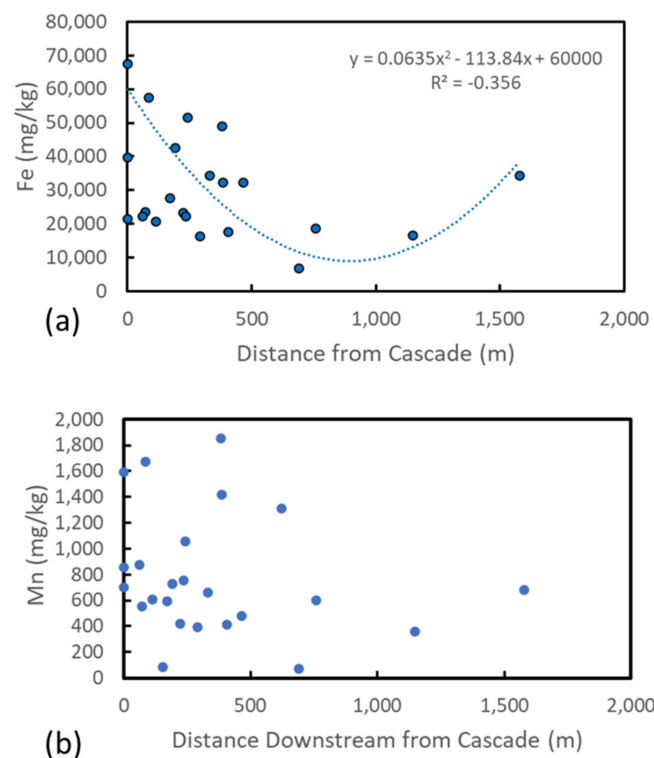


Figure 9. Variations in Fe (a) and Mn (b) concentrations as a function of downstream distance from a cascade. No statistically significant relationship exists for Mn.

With a few exceptions [40,46], neither fine sediment nor trace metal partitioning into channel bed features along bedrock rivers have been extensively studied. Skalak and Pizzuto [46] found, however, that along the South River of Virginia, sand, silt, clay, and organic matter were preferentially deposited in what they referred to as fine-grained channel margin deposits. These deposits formed in areas of relatively slow-moving water in the wake of large woody debris that obstructed flow. Accumulations of large woody debris are rare along the SFNR. The primary obstructions to flow are created by the bedrock ribs that traverse the channel perpendicular to flow and that form the cascades. Sand and coarser sediments have accumulated both up- and downstream of nearly all transverse ribs (Figure 8). Such topographic features along bedrock channels have been shown to increase form drag [47,48], which may locally reduce the flows sediment transport capacity and result in local sediment deposition [11,49]. In fact, Goode and Wohl [49] found that discontinuous patches of alluvial sediments were commonly located within topographic lows between consecutive downstream ribs, and in the wake of the bedrock ribs, as shown in Figure 8 for the SFNR. Site NR 26, for example, is located immediately downstream of a bedrock rib in a zone of relatively quiet water (Figure S3). These sediments contain relatively high quantities of fine sediment (Figure 4a,b). Interestingly, at Site NR 4, the pool is relatively deep, and the channel bifurcates around an island immediately downstream; the island abruptly terminates at a bedrock rib that forms a small cascade that has locally reduced flow velocities (Figure S4). Similarly, at NR 21, the sampling site is again located immediately upstream of a bedrock obstruction that forms a cascade that has locally disrupted flow (Figure S3). It appears, then, that localized zones of sediment deposition may not only occur downstream of the bedrock ribs, but upstream where flow is diverted toward topographic lows along the rib. It is also possible, as suggested by the theoretical work of Nelson and Seminara [10] that once sediment deposition has been initiated, differences in hydraulic roughness between the exposed bedrock and the sediment will allow the sediment to become locally concentrated. Regardless of the exact mechanism, the transverse bedrock ribs are a primary driver of localized sediment deposition, including relatively fine-grained sediments.

At a larger scale, trace metals as well as Mn and Fe concentrations were elevated in pools located downstream of a few, but not all, cascades (e.g., Sites NR 8–10, NR 21, NR 26, Figure 4c). Thus, we hypothesized that pools would, in general, possess larger quantities of fine sediments and/or heavy mineral grains. To test these hypotheses, a Mann–Whitney U test was used to compare the quantities (%) of fine sediment, organic matter, and metal (Cr, Cu, Fe, Mn, Zn) concentrations between samples collected from the pools and bedrock reaches. The analysis suggests that there is no difference in these parameters between the two reach types at the 95% confidence level over the entire study reach (Table S6). While the pools accumulate slightly more unconsolidated sediment, trace metal concentrations do not appear to be statistically influenced by the preferential deposition of either fine-sediment or heavy mineral grains within the pool reaches.

4.2.3. Reach-Scale Geomorphic Influences on Downstream Variations in Metal Concentrations

In addition to the localized partitioning of trace metals into specific geomorphic channel bed features (e.g., pools, bars, and riffles), previous studies of alluvial rivers have shown that chemically reactive fine-grained sediments can be preferentially deposited along specific, larger-scale stream segments. The most commonly observed trend is for enhanced deposition to occur along relatively wide, low-gradient valleys, referred to as depositional zones; narrow valleys characterized by relatively steep slopes are conducive to sediment transport (and have been called transport zones) [28,50]. Here, we assessed the potential influence of downstream variations in channel and valley morphology on the deposition and storage of reactive sediments and the trace metals that they may contain using principal component analysis (PCA). Channel characteristics were characterized in terms of channel width and slope, whereas valley morphology was characterized by valley width. In addition, the concentrations of the trace metals examined herein (Cr, Cu, Zn), were included in the analysis, along with Mn, Fe, Al, and Si which were used to represent chemically reactive constituents in the channel bed sediments. The data were standardized prior to analysis to account for differences in parameter units.

The first two components of the analysis explained 64.4% of the variation in the data. Component 1 (Figure 10a) possessed high positive loadings for all of the included trace metals (Cu, Cr, and Zn), as well as for Mn, Fe, and Al (Table 3). Si exhibited a strong negative score on Component 1. These data support our earlier analyses that indicate that the trace metals are primarily associated with Fe and Mn compounds and, to a lesser degree, fine-grained sediments. Both channel width and slope had high positive scores on Component 2; valley width exhibited a relatively high negative score on Component 2. These loadings indicate that narrow valleys tended to possess wider, higher gradient channels. Interestingly, Al, but not Si, exhibited a relatively high score on Component 2. It is not entirely clear why this relation exists, but low negative Si loadings on Component 2 suggests that it is not entirely related to the grain size of the sediment.

The joint downstream variations in sediment composition can be examined with respect to channel and valley form by plotting the component scores along the study reach (Figure 10b). High Component 1 scores are indicative of reaches characterized by relatively high trace metal concentrations, as well as fine sediment, Mn, and Fe contents. In contrast, low Component 2 scores indicate relatively narrow, lower gradient channels, in wider valleys. Figure 10b shows that reaches with increased Fe and Mn concentrations (e.g., sites NR 9, 10, 21) and/or fine sediment (e.g., Site NR 21) are characterized by low Component 2 scores. This inverse relation does not exist at most other sampling sites. Nonetheless, these results indicate that there is a tendency for fine sediment to accumulate along wider, lower gradient stream reaches along part, but not all, of the study reach. It appears, then, that reaches possessing anomalously high trace metal, Mn, and Fe contents within the study area of the SFNR are influenced not only by their location downstream of cascades composed of rather unique bedrock, but by river reaches characterized by relatively narrow, low gradients channels (with presumably deeper water) within wider valleys.

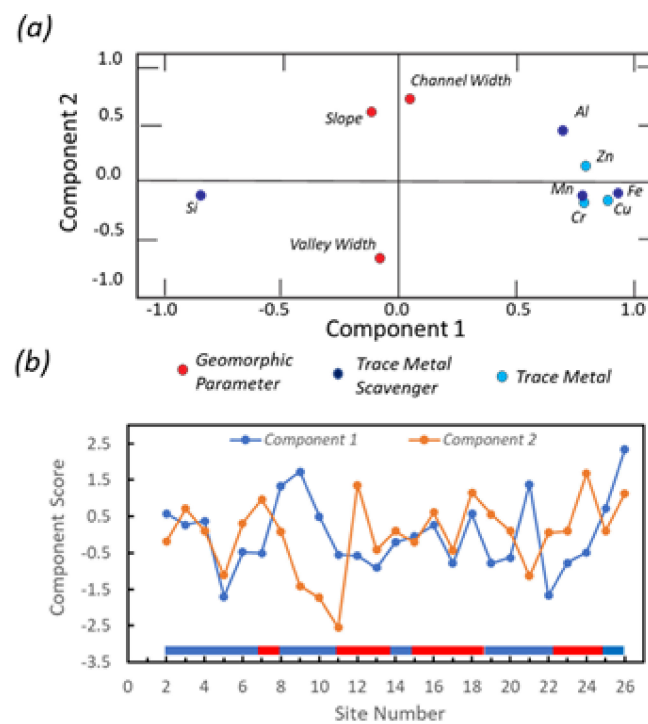


Figure 10. (a) Plot of Component 1 and Component 2 loadings showing general relationships between the parameters; (b) Downstream variations in component 1 and 2 scores. High Component 1 scores indicate relatively high metal concentrations, a high percentage of fine sediment and high organic matter contents. High Component 2 scores are suggestive of narrow, low-gradient channels in wide valleys. Larger tributaries are shown by red arrows. Colored bar shows distribution of pool (blue) and shallow bedrock (red) reaches.

Table 3. Summary of Component Loadings.

Variable	Comp. 1	Comp. 2
Channel Width	0.034	0.716
Valley Width	−0.085	−0.709
Channel Slope	−0.122	0.622
Al	0.681	0.439
Cu	0.887	−0.160
Cr	0.779	−0.214
Fe	0.933	−0.125
Mn	0.774	−0.152
Si	−0.852	−0.140
Zn	0.790	0.145

Bold—high loadings on component.

5. Summary and Conclusions

This study examined the factors controlling the downstream variations in selected toxic trace metal (Cr, Cu, Zn) concentrations along the bedrock dominated channel of the South Fork New River (SFNR). The topography of the channel bed, and thus its hydraulic roughness, is highly variable, but elevated along localized reaches of cascades consisting of topographic ridges (ribs) separated by topographic lows that are oriented perpendicular to flow. The accumulation of channel bed sediment does not occur in a repetitive, systematic pattern along the channel as is typical of alluvial rivers. Rather, patches of alluvial sediments are primarily associated with transverse ribs that obstruct flow, and that create zones of localized quiet water up, within, and downstream of the cascades. Trace metal concentrations along the river generally vary within a narrow range of background values, but are locally elevated within a few, short reaches. Stream

segments with elevated trace metal contents also possess high concentrations of Mn and Fe, suggesting that the trace metals are primarily associated with Mn and Fe bearing heavy minerals and/or oxyhydroxides. Chemically reactive fine-grained (<63 µm) sediments have a more limited influence on the downstream variations in metal concentrations, presumably because the channel bed sediments are composed primarily of sand-sized and larger particles. In fact, fine sediment comprised <5% of the bed sediment at most sampling sites.

Reaches of elevated metal concentration (e.g., at Sites NR 8–10, 21, and NR 25–26) are located within deeper, low velocity waters within the cascades, or within reach-scale pools located immediately downstream of bedrock cascades containing transversely oriented ribs. We believe that localized zones of metal enrichment result from the erosion of lithologic units within the cascades that contain sulfidic layers or zones of mafic mineral enrichment, which are known to occur in the underlying bedrock. Once eroded, these minerals and/or rock fragments are subsequently deposited within pools, including pools located along channel reaches that, according to a PCA, possess relatively wide valleys and low channel gradients. The enrichment of trace metals downstream of the cascades may also be due to the oxidation of Fe and Mn (forming Fe and Mn oxyhydroxides) as river water is aerated by turbulence as it flows over and through the cascades.

The localized variations in trace metal concentrations related to the cascades and the patchwork of accumulated sediments can increase field variance, which Birch et al. [50] defined as the variations in concentrations over a short-section of the stream channel. Increased field variance can greatly reduce our ability to decipher downstream patterns in metal concentrations that may be indicative of a contaminant source(s), particularly where the rivers are only slightly contaminated [50]. It is important, then, for the design of future sampling programs to take the potential for localized variations in trace metal concentrations created by the variations in channel bed topography (cascades, pools) into consideration along such bedrock-controlled, coarse-grained channels.

Supplementary Materials: The following are available online at <https://www.mdpi.com/article/10.3390/geosciences11120519/s1>, Figure S1: Illustration of the methods used to characterize channel and valley morphology; Figure S2: Images of bedrock reaches along the SFNR; Table S1: Descriptive statistics for selected geochemical and grain size parameters; Table S2: Manning–Whitney U test results of statistical differences in metal concentrations between background and potentially mine contaminated sites; Table S3: Emergency Response Actions taken by USEPA at the Ore Knob Mine; Table S4: General description of geologic units underlying SFNR; Table S5: Kruskal–Wallis test results of statistical differences in geochemistry between reaches underlain by different bedrock units. Figure S3: Aerial images of sampling sites NR 21 and NR 26; Figure S4: Aerial images of sampling sites for NR 3; Table S6: Manning–Whitney U test results of statistical differences in metal concentrations between pool and bedrock reaches.

Author Contributions: Conceptualization, J.R.M.; methodology, J.R.M., X.W.; formal analysis, X.W. (geochemical and sedimentological analyses); T.O. (Cartographic/GIS analyses); investigation, J.R.M., X.W., T.O., C.A.; resources, J.R.M.; data curation, J.R.M.; writing—original draft preparation, J.R.M.; writing—review and editing, J.R.M., X.W., T.O., C.A.; supervision, J.R.M., C.A.; funding acquisition, J.R.M. All authors have read and agreed to the published version of the manuscript.

Funding: This research was funded by the Whitmire Endowment at Western Carolina University.

Institutional Review Board Statement: Not applicable.

Informed Consent Statement: Not applicable.

Data Availability Statement: The data presented in this study are available on request from the corresponding author. Data that are publicly available are in the paper or in Supplemental Materials.

Acknowledgments: Gina Carney and Lionel Villarroel aided in the collection of the sediment samples and other field data. The authors greatly appreciate their help. We also thank Thomas Martin for his help in conducting the robust least trimmed square regression analysis using R programming

language. The manuscript benefitted greatly from the comments of three anonymous reviewers. We greatly appreciated their effort to improve upon the paper.

Conflicts of Interest: The authors declare no conflict of interest.

References

- Macklin, M.G. Metal Contaminated Soil and Sediment: A Geographical Perspective. In *Managing the Human Impact on the Natural Environment: Patterns and Processes*; Newson, M.D., Ed.; Belhaven Press: London, UK, 1992; pp. 174–195.
- Macklin, M.G.; Brewer, P.A.; Hudson-Edwards, K.A.; Bird, G.; Coulthard, T.J.; Dennis, I.A.; Lechler, P.J.; Miller, J.R.; Turner, J.N. A Geomorphological Approach to the Management of Rivers Contaminated by Metal Mining. *Geomorphology* **2006**, *79*, 423–447. [[CrossRef](#)]
- Miller, J.R.; Orbock Miller, S.M. *Contaminated Rivers: A Geomorphological-Geochemical Approach to Site Assessment and Remediation*; Springer Science & Business Media: Berlin/Heidelberg, Germany, 2007; ISBN 9781402056024.
- Matys Grygar, T.; Elznicová, J.; Tůmová, Š.; Faměra, M.; Balogh, M.; Kiss, T. Floodplain Architecture of an Actively Meandering River (the Ploučnice River, the Czech Republic) as Revealed by the Distribution of Pollution and Electrical Resistivity Tomography. *Geomorphology* **2016**, *254*, 41–56. [[CrossRef](#)]
- Matys Grygar, T.; Elznicová, J.; Bábek, O.; Hošek, M.; Engel, Z.; Kiss, T. Obtaining Isochrones from Pollution Signals in a Fluvial Sediment Record: A Case Study in a Uranium-Polluted Floodplain of the Ploučnice River, Czech Republic. *Appl. Geochem.* **2014**, *48*, 1–15. [[CrossRef](#)]
- Hudson-Edwards, K.A.; Jamieson, H.E.; Lottermoser, B.G. Mine Wastes: Past, Present, Future. *Elements* **2011**, *7*, 375–380. [[CrossRef](#)]
- Miller, J.R.; Lechler, P.J.; Desilets, M. The Role of Geomorphic Processes in the Transport and Fate of Mercury in the Carson River Basin, West-Central Nevada. *Environ. Geol.* **1998**, *33*, 249–262. [[CrossRef](#)]
- Horowitz, A.J.; Elrick, K.A. The Relation of Stream Sediment Surface Area, Grain Size and Composition to Trace Element Chemistry. *Appl. Geochem.* **1987**, *2*, 437–451. [[CrossRef](#)]
- Martin, J.-M.; Meybeck, M. Elemental Mass-Balance of Material Carried by Major World Rivers. *Mar. Chem.* **1979**, *7*, 173–206. [[CrossRef](#)]
- Nelson, P.A.; Seminara, G. A Theoretical Framework for the Morphodynamics of Bedrock Channels. *Geophys. Res. Lett.* **2012**, *39*, 30. [[CrossRef](#)]
- Inoue, T.; Izumi, N.; Shimizu, Y.; Parker, G. Interaction among Alluvial Cover, Bed Roughness, and Incision Rate in Purely Bedrock and Alluvial-Bedrock Channel. *J. Geophys. Res. Earth Surf.* **2014**, *119*, 2123–2146. [[CrossRef](#)]
- Goode, J.R.; Wohl, E. Coarse Sediment Transport in a Bedrock Channel with Complex Bed Topography. *Water Resour. Res.* **2010**, *46*, 22. [[CrossRef](#)]
- Finnegan, N.J.; Sklar, L.S.; Fuller, T.K. Interplay of Sediment Supply, River Incision, and Channel Morphology Revealed by the Transient Evolution of an Experimental Bedrock Channel. *J. Geophys. Res. Earth Surf.* **2007**, *112*, 134. [[CrossRef](#)]
- Whipple, K.X. Bedrock rivers and the geomorphology of active orogens. *Annu. Rev. Earth Planet. Sci.* **2004**, *32*, 151–185. [[CrossRef](#)]
- Sklar, L.S.; Dietrich, W.E. Sediment and Rock Strength Controls on River Incision into Bedrock. *Geology* **2001**, *29*, 1087–1090. [[CrossRef](#)]
- Custer, K. *Cleaning Up Western Watersheds: A Report by Kelly Custer for Mineral Policy Center*; U.S. Environmental Protection Agency: Washington, DC, USA, 2003; p. 36.
- USEPA Mine Sites: Characterization, Cleanup, and Revitalization of Mine Sites. *Contaminated Site Clean-Up Information*; USEPA: Washington, DC, USA, 2021.
- Behrooz, M. Acid Mine Drainage at Ore Knob Tailings Pile-Hydrologic and Geochemical Characterization and Bioremediation. Ph.D. Thesis, North Carolina State University, Raleigh, NC, USA, 2012.
- Rankin, H.S.; Stuckey, J.L. *Copper Deposits of Western North Carolina*; TVA and NC Division of Mineral Resources: Knoxville, TN, USA, 1943.
- Kinkel, A.R., Jr. *The Ore Knob Copper Deposit North Carolina, and Other Massive Sulfide Deposits of the Appalachians*; USGS Professional Paper: Washington, DC, USA, 1967.
- Ore Knob Mine NPL Site. *NCDHHS Public Health Assessment*; NCDHHS: Raleigh, NC, USA, 2010.
- NCOneMap. NC OneMap: Geology. 2009. Available online: <https://www.nconemap.gov/> (accessed on 1 December 2021).
- FRIS. North Carolina Flood Risk Information System. Available online: <https://fris.nc.gov/fris/Index.aspx?ST=NC> (accessed on 1 December 2021).
- Horowitz, A.J. *Primer on Sediment-Trace Element Chemistry*; Lewis Publishers: Boca Raton, FL, USA, 1991; ISBN 9780873714990.
- Evans, D.; Davies, B.E. The Influence of Channel Morphology on the Chemical Partitioning of Pb and Zn in Contaminated Rivers. *Appl. Geochem.* **1994**, *9*, 45–52. [[CrossRef](#)]
- Ciszewski, D. Source of Pollution as a Factor Controlling Distribution of Heavy Metals in River Chechlo Bottom Sediments. *Environ. Geol.* **1997**, *28*, 50–57. [[CrossRef](#)]
- Balaban, S.-I.; Hudson-Edwards, K.A.; Miller, J.R. A GIS-Based Method for Evaluating Sediment Storage and Transport in Large Mining-Affected River Systems. *Environ. Earth Sci.* **2015**, *74*, 4685–4698. [[CrossRef](#)]

28. Hoogsteen, M.J.J.; Lantinga, E.A.; Bakker, E.J.; Groot, J.C.J.; Tittonell, P.A. Estimating Soil Organic Carbon through Loss on Ignition: Effects of Ignition Conditions and Structural Water Loss. *Eur. J. Soil Sci.* **2015**, *66*, 320–328. [[CrossRef](#)]
29. Macklin, M.G. Fluxes and Storage of Sediment-Associated Heavy Metals in Floodplain Systems: Assessment and River Basin Management Issues at a Time of Rapid Environmental Change. In *Floodplain Processes*; Anderson, M.G., Walling, D.E., Bates, P.B., Eds.; John Wiley & Sons, Ltd.: Hoboken, NJ, USA, 1996; pp. 441–446.
30. Bábek, O.; Grygar, T.M.; Faměra, M.; Hron, K.; Nováková, T.; Sedláček, J. Geochemical Background in Polluted River Sediments: How to Separate the Effects of Sediment Provenance and Grain Size with Statistical Rigour? *CATENA* **2015**, *135*, 240–253. [[CrossRef](#)]
31. Segeman, B.B.; Lyons, T.W. Geochemistry of Fine-Grained Sediments and Sedimentary Rocks. In *Sediments, Diagenesis, and Sedimentary Rocks*; Treatise on Geochemistry; Mackenzie, F.T., Ed.; Elsevier: Amsterdam, The Netherlands, 2005; pp. 115–289.
32. Bloemsmá, M.R.; Zabel, M.; Stuut, J.B.W.; Tjallingii, R.; Collins, J.A.; Weltje, G.J. Modelling the Joint Variability of Grain Size and Chemical Composition in Sediments. *Sediment. Geol.* **2012**, *280*, 135–148. [[CrossRef](#)]
33. Tukey, J.W. *Exploratory Data Analysis*; Addison Wesley: Boston, MA, USA, 1977.
34. Reimann, C.; Garrett, R.G. Geochemical Background—Concept and Reality. *Sci. Total Environ.* **2005**, *350*, 12–27. [[CrossRef](#)]
35. Dendievel, A.-M.; Mourier, B.; Dabrin, A.; Delile, H.; Coynel, A.; Gosset, A.; Liber, Y.; Berger, J.-F.; Bedell, J.-P. Metal Pollution Trajectories and Mixture Risk Assessed by Combining Dated Cores and Subsurface Sediments along a Major European River (Rhône River, France). *Environ. Int.* **2020**, *144*, 106032. [[CrossRef](#)]
36. Woldfenden, P.I.; Lewin, J. Distribution of Metal Pollution in Floodplain Sediments. *CATENA* **1977**, *4*, 309–317. [[CrossRef](#)]
37. Lewin, J.; Macklin, M. Metal Mining and Floodplain Sedimentation in Britain. In *International Geomorphology*; Part I; Garkiner, V., Ed.; John Wiley & Sons, Ltd.: Hoboken, NJ, USA, 1987.
38. Taylor, M.P.; Kesterton, R.G.H. Heavy Metal Contamination of an Arid River Environment: Gruben River, Namibia. *Geomorphology* **2002**, *42*, 311–327. [[CrossRef](#)]
39. USEPA. *Final Expanded Site Inspection Report Ore Knob Former Mine Site, Ashe County, North Carolina*; CERCLIS: Atlanta, GA, USA, 2008.
40. Miller, J.R.; Mackin, G. Concentrations, Sources, and Potential Ecological Impacts of Selected Trace Metals on Aquatic Biota within the Little Tennessee River Basin, North Carolina. *Water Air Soil Pollut.* **2013**, *224*, 1613. [[CrossRef](#)]
41. North Carolina Geological Survey, (NCGS). *Acidic Rocks in the Little Tennessee River Basin*; NCGS: Raleigh, NC, USA, 1985.
42. Jankowski, J. Changes in Water Quality in a Stream Impacted by Longwall Mining Subsidence. In Proceedings of the 7th Triennial Conference on Mine Subsidence; Mine Subsidence Technological Society, Wollongong, Australia, 26–27 November 2007; pp. 241–251.
43. Ladd, S.C.; Marcus, W.A.; Cherry, S. Differences in Trace Metal Concentrations among Fluvial Morphic Units and Implications for Sampling. *Environ. Geol.* **1998**, *36*, 259–270. [[CrossRef](#)]
44. Ciszewski, D. Pollution of Mala Panew River Sediments by Heavy Metals: Part I. Effect of Changes in River Bed Morphology. *Pol. J. Environ. Sci. Stud.* **2004**, *13*, 589–595.
45. Graf, W.L.; Clark, S.L.; Kammerer, M.T.; Lehman, T.; Randall, K.; Schroeder, R. Geomorphology of Heavy Metals in the Sediments of Queen Creek, Arizona, USA. *CATENA* **1991**, *18*, 567–582. [[CrossRef](#)]
46. Skalák, K.; Pizzuto, J. The Distribution and Residence Time of Suspended Sediment Stored within the Channel Margins of a Gravel-Bed Bedrock River. *Earth Surf. Process. Landf.* **2010**, *35*, 435–446. [[CrossRef](#)]
47. Wohl, E.E.; Ikeda, H. Experimental Simulations of Channel Incision into a Cohesive Substrate at Varying Gradients. *Geology* **1997**, *25*, 295–298. [[CrossRef](#)]
48. Johnson, J.P.; Whipple, K.X. Feedbacks between Erosion and Sediment Transport in Experimental Bedrock Channels. *Earth Surf. Process. Landf.* **2007**, *32*, 1048–1062. [[CrossRef](#)]
49. Goode, J.R.; Wohl, E. Substrate Controls on the Longitudinal Profile of Bedrock Channels: Implications for Reach-Scale Roughness. *J. Geophys. Res. Earth Surf.* **2010**, *115*, 69. [[CrossRef](#)]
50. Birch, G.F.; Taylor, S.E.; Matthai, C. Small-Scale Spatial and Temporal Variance in the Concentration of Heavy Metals in Aquatic Sediments: A Review and Some New Concepts. *Environ. Pollut.* **2001**, *113*, 357–372. [[CrossRef](#)]